Int. J. Solids Structures, 1972, Vol. 8, pp. 1299 to 1318. Pergamon Press. Printed in Great Britain

PLASTIC LIMIT BEHAVIOR AND FAILURE OF FILAMENT REINFORCED MATERIALS

P. V. MCLAUGHLIN, JR.

Department of Theoretical and Applied Mechanics, University of Illinois, Urbana, Illinois 61801

Abstract—Plane stress limit conditions or maximum plastic strength envelopes are derived using limit analysis for arbitrary planar arrays of thin, strong filaments in a matrix of weaker material. Both filaments and matrix are assumed plastic with acceptable limit behavior, but respective limit conditions are arbitrary. The limiting case of a volume fraction weighted average of the constituent phase limit stresses is predicted for plastic composite strength, which should also be an upper bound to strength of composites with brittle filaments or where fracture can otherwise occur. Specific results are given for unidirectional and bidirectional reinforcement which agrees with experiment.

INTRODUCTION

THE ability to tailor mechanical and thermal properties of structures to obtain optimum performance using fiber reinforced materials is well known. In addition to widely used high-strength, brittle reinforcement, many applications include fibers which behave plastically. Examples of these materials are steel or copper wire reinforced solid rocket propellant, steel wire reinforced epoxy, high strength polymer reinforced plastics, and tungsten wire reinforced copper (see Refs. [1, 2] for others). In a previous paper, McLaughlin and Batterman [3] presented the basic theory for computing plane stress limit surfaces or maximum plastic strength envelopes for planar arrays of perfectly plastic filaments using limit analysis [4, 5] techniques. A basic assumption in the McLaughlin–Batterman work [3] was the neglect of matrix strength in comparison to that of the filaments. It is the purpose of the present paper to use limit analysis [4–6] to predict plastic (limit) strength of planar filamentary composites having matrix materials that contribute significantly to composite strength.

Hashin [7], Shu and Rosen [8] and others have used limit analysis techniques to determine limit strengths in axial and transverse tension and shear of a unidirectionally reinforced composite. Multiaxial reinforcement was not considered, however, and determination of complete limit surfaces was not attempted. General yield and stress–strain behavior of unidirectional inextensible or elastic reinforcement of a plastic matrix has been discussed by Mulhern *et al.* [9 and others]. Prager [10] considered the specific case of reinforcement of a rigid-plastic von Mises matrix with one and two families of infinite strength, inextensible filaments by investigating the restrictions thereby imposed on matrix deformation. Helfinstine and Lance [11] attempted a similar analysis for a matrix material obeying the Tresca or maximum shear stress criterion. Lance and Robinson [12] have proposed a semi-empirical theory of failure of uniaxially reinforced, perfectly plastic fiber-and-matrix composites based on phase geometry and principles of the theory of plasticity. Also, elementary predictions of the tensile strength of filament composites has been given, for example, by Stowell and Liu [13] and Kelly and Tyson [14].

It should be mentioned that other researchers (Azzi and Tsai [15] and Chamis [16] for example) have proposed anisotropic failure surfaces which can be used to good advantage in empirically representing yield or limit surfaces for composites. The "other ended" approach given here is geared to provide qualitative insight into constituent geometrical and material effects on composite behavior as well as provide a means of quantitative prediction for material and structural design.

Since many filamentary composites see structural application under plane loading conditions, composite limit conditions are developed in plane stress. While matrix and filament material is otherwise arbitrary, both phases will be assumed plastic with filaments considerably stronger than the matrix. It is emphasized that the composite limit conditions are not, in general, yield conditions [6] except in the many times useful idealization of rigid-perfect plasticity. In the present analysis, material behavior is not restricted to rigid-perfect plasticity, but must exhibit ductile limit behavior [6]. Infinite strength or inextensible filaments are included by letting filament limit strength approach infinity. Even though the present analysis is for plastic limit behavior, it is expected that its strength prediction will be an upper bound to strength of brittle filament reinforced ductile matrices or composites which otherwise fail by filament, matrix or bond separation.

The next section of this paper presents the limit behavior of planar multidirectionally reinforced materials having arbitrary fiber orientation and material limit conditions. An example illustrates application of the derived equations, and infinite strength inextensible filaments are discussed. Because of the wide usage of unidirectionally and bidirectionally reinforced composites, their strength properties are given in the following section. Finally, the upper bound relationship of the limit theory to strength of composites which fail by fracture or separation of filaments, matrix or interface bounds is discussed.

GENERAL LIMIT BEHAVIOR

The composite material under consideration is composed of a planar array of an arbitrary number of filaments imbedded at different angles in a matrix. Both filament and matrix materials are plastic and have unique limit [4–6] surfaces in stress space under general three dimensional states of stress where continued plastic deformation can occur under no increase in stress, Fig. 1. Initial work-hardening of both filaments and matrix is

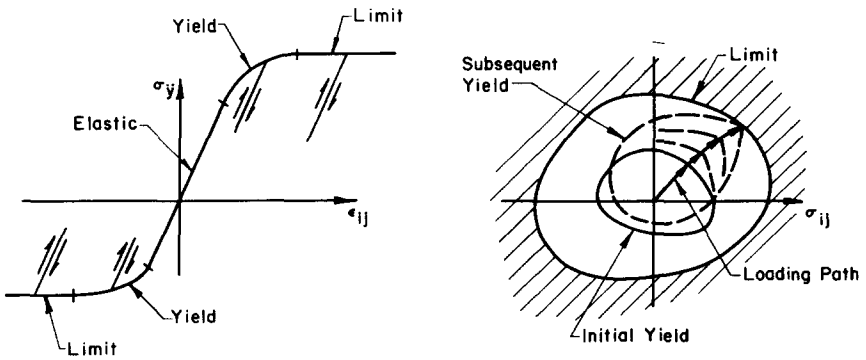

FIG. 1. Schematic of material behavior which is acceptable for limit analysis.

allowed to the extent described in [6]. The composite is therefore acceptable for application of limit analysis [4] which is the analytical tool used herein to derive combinations of maximum plastic stress, or limit conditions, for the composite as a whole.

In practice, filament reinforcement is almost always considerably stronger than the matrix material. Matrix strength in the limit sense will therefore be assumed much less than that of the filaments, giving maximum stress levels in the matrix which are considerably less than stresses in the fibers. Under these conditions it is reasonable to assume that limit stresses in the fiber are primarily uniaxial tension and compression and are unaffected by matrix stresses.

Both actual and assumed compatible deformations in a composite can be complex and dependent on phase geometry and volume fractions as well as material properties. To simplify the analysis, the filaments will be assumed infinitesimally thin, with all material concentrated along their axes.

The limit surface

A representative structural element (RSE) of filamentary composite is shown in Fig. 2. Cartesian axes x_1, x_2, x_3 are fixed in the center of the RSE which has unit dimensions in

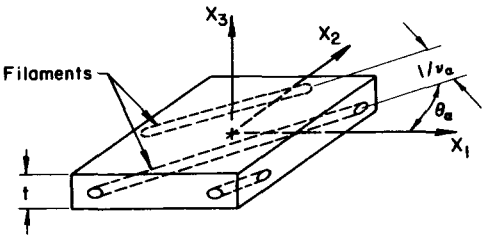

(a) Dimensions, Filament Orientation And Number Density

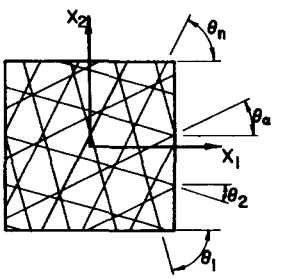

(b) Filament Family Numbering Convention

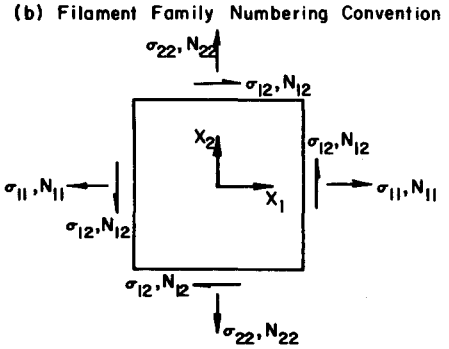

(c) Stresses And Membrane Force Resultants

FIG. 2. Representative structural element of filamentary composite.

the x_1 and x_2 directions, but thickness t in the x_3 direction. An angle θ defined between $-\pi/2$ and $\pi/2$ and measured positive counterclockwise from the x_1 axis, gives the orientation of the filaments in the RSE. There are n families of filaments, all ath family filaments having orientation θ_a spacing $1/v_a$ and extremely small cross sectional area A_a. The number of filaments per unit length perpendicular to the filament axis is v_a. It follows from [3] that the volume fraction of filaments is, using the summation convention for repeated subscripts,

$$v^f = A_a v_a / t \ll 1 \qquad (a = 1, \ldots, n) \tag{1a}$$

and volume fraction of matrix is, due to the smallness of v^f,

$$v^m = 1 - A_a v_a / t \cong 1. \tag{1b}$$

The ath filament limit stress in tension and compression will be denoted σ_a^0 and $\phi_c^{(a)}\sigma_a^0$, respectively, where $\phi_c^{(a)}$ is a positive constant and can be greater or less than unity. The stress σ_a^0 is assumed very large such that filament strength $f_a^0 = \sigma_a^0 A_a$ remains finite as A_a becomes negligible.

It will later prove useful to have the plane stress limit surface for the filamentary array alone without the matrix material, i.e. for zero matrix strength. This surface has been computed for arbitrary filament orientation in Ref. [3] to which the reader is referred for more detail. Results are given in terms of normal (N_{11}, N_{22}) and shear (N_{12}) membrane forces/unit length. Let this limit surface be denoted

$$L^f(N_{11}, N_{22}, N_{12}) = 0, \qquad N_{ij} = N_{ij}^{Lf} \qquad (i, j = 1, 2) \tag{2}$$

where force points on the surface are denoted N_{ij}^{Lf}. Force points outside the surface (2) are not allowed.

Similarly, let the limit surface for the matrix material under general stress be given by

$$L^m(\sigma_{11}, \ldots, \sigma_{23}), \qquad \sigma_{ij} = \sigma_{ij}^{Lm} \qquad (i, j = 1, 2, 3) \tag{3}$$

where σ_{ij}^{Lm} represent points on the matrix limit surface and points outside the surface are not allowed.

Computation of an upper bound [4] to the composite limit surface requires assuming a kinematically admissible velocity field, computing the rate of internal work

$$D = \int_V \sigma_{ij}\varepsilon_{ij}\,\mathrm{d}V = \int_{V^m} \sigma_{ij}^m \varepsilon_{ij}^m\,\mathrm{d}V + \int_{V^f} \sigma_{ij}^f \varepsilon_{ij}^f\,\mathrm{d}V, \tag{4}$$

(no discontinuities)

and equating it to the rate of external work

$$W = \int_S T_i v_i\,\mathrm{d}S \tag{5}$$

where $\sigma_{ij}, \varepsilon_{ij}$ are stresses and strain rates, respectively, in the RSE of volume V; T_i, v_i are surface tractions and velocities, respectively, on the RSE external surface S. The superscripts m and f denote quantities pertaining to matrix and filaments, respectively. Let the velocity field be linear such that constant strain rates $\varepsilon_{ij} = \overset{*}{\varepsilon}_{ij}$ exist throughout the matrix. Moreover, the $\overset{*}{\varepsilon}_{ij}$ are chosen from the requirement of normality of the strain rate vector to the limit surface [4, 6], to correspond to some point $\sigma_{11} = \overset{*}{\sigma}_{11}^{Lm}, \sigma_{22} = \overset{*}{\sigma}_{22}^{Lm}, \sigma_{12} = \overset{*}{\sigma}_{12}^{Lm}, \sigma_{13} = \sigma_{23} =$

$\sigma_{33} = 0$ on the matrix limit surface (3). This gives, for the rate of internal work of the matrix,

$$\int_{V^m} \sigma_{ij}^m \dot{\varepsilon}_{ij}^m \, dV = (\dot{\bar{\sigma}}_{11}^{Lm} \dot{\bar{\varepsilon}}_{11} + \dot{\bar{\sigma}}_{22}^{Lm} \dot{\bar{\varepsilon}}_{22} + 2\dot{\bar{\sigma}}_{12}^{Lm} \dot{\bar{\varepsilon}}_{12}) t v^m. \tag{6}$$

By virtue of the assumed infinitessimal cross sectional dimensions of the filaments, the deformation rates in the filaments can be purely axial without affecting continuity of velocity. Under these conditions, the rate of internal work of the filaments is, from [3],

$$\begin{aligned} \int_{V^f} \sigma_{ij}^f \dot{\varepsilon}_{ij}^f \, dV &= \sum_{a=1}^{n} \int_{V_a^f} \sigma_a e_a \, dV \\ &= \dot{\bar{\varepsilon}}_{11} \sum_{a=1}^{n} f_a v_a \cos^2\theta_a + \dot{\bar{\varepsilon}}_{22} \sum_{a=1}^{n} f_a v_a \sin^2\theta_a \\ &\quad + 2\dot{\bar{\varepsilon}}_{12} \sum_{a=1}^{n} f_a v_a \sin\theta_a \cos\theta_a \\ &= \dot{N}_{ij}^{Lf} \dot{\bar{\varepsilon}}_{ij} \qquad (i, j = 1, 2). \end{aligned} \tag{7}$$

Here σ_a and f_a are the uniaxial filament stresses and forces, respectively, determined by the uniaxial filament strain rate e_a which in turn depends on $\dot{\bar{\varepsilon}}_{ij}$. The $\dot{N}_{ij}^{Lf}$ correspond to particular stress points on the "filament alone" limit surface, equation (2), where the normal to the surface has components proportional to $\dot{\bar{\varepsilon}}_{11}, \dot{\bar{\varepsilon}}_{22}, \dot{\bar{\varepsilon}}_{12}$ in the $N_{11}^{Lf}, N_{22}^{Lf}, N_{12}^{Lf}$ directions, respectively.

The rate of external work, equation (5), reduces to

$$W = \bar{\sigma}_{ij} \dot{\bar{\varepsilon}}_{ij} t \qquad (i, j = 1, 2). \tag{8}$$

$\bar{\sigma}_{ij}$ is the average or effective composite stress and is given by the total force in the x_i direction on an RSE coordinate surface orthogonal to x_j divided by the RSE coordinate surface area S_j:

$$\bar{\sigma}_{ij} = \frac{1}{t} \int_{S_j} T_i \, dS_j \qquad (i, j = 1, 2, \text{no sum}). \tag{9}$$

Upon substituting equations (6) and (7) into (4), equating (4)–(8), and noting that the coefficients $\dot{\bar{\varepsilon}}_{ij}$ are arbitrary, we get an upper bound to the composite limit surface in terms of limit properties of the constituents:

$$\bar{\sigma}_{ij} = \dot{\bar{\sigma}}_{ij}^{Lm} + \frac{\dot{N}_{ij}^{Lf}}{t} \qquad (i, j = 1, 2) \tag{10}$$

where the approximation $v^m \cong 1$ has been used. It is noted again that the $\dot{\bar{\sigma}}_{ij}^{Lm}$ are points on the matrix and "filament alone" limit surfaces, respectively, where surface normal vector components are proportional to $\dot{\bar{\varepsilon}}_{ij}$.

A lower bound [4] to the composite limit surface is obtained by assuming an equilibrium stress field in the composite which is everywhere at or below limit in both phases and calculating the resultant external forces. It is convenient to choose the state of stress $\dot{\bar{\sigma}}_{ij}^{Lm}$ in the matrix which corresponds to the point on the matrix limit surface where the normal to the surface has components $\dot{\bar{\varepsilon}}_{ij}$. Shear and normal stresses need be continuous across the

matrix–filament interface, but the axial filament stress can be chosen separately from the same stress component in the surrounding matrix. Hence, a filament stress field is chosen which is equal to the matrix stress field in a filament axis coordinate system except for the component along the filament axis. Each family's axial stress is chosen to give "filament alone" resultant forces of $\mathring{N}_{ij}^{Lf}$ (by assumption, matrix stresses have negligible effect on filament yielding). The resulting lower bound to the limit surface is found from equation (9) to be precisely equation (10), previously obtained as an upper bound. Since the upper and lower bounds coincide, it is concluded that equation (10) is the limit surface for the filamentary composite.

Flow law

The stress–strain relationships or flow laws for plastic materials are discussed by Drucker [17], and for general composite materials by Hill [18]. In these papers, it is shown that for materials, structures and composite materials which obey certain stability criteria [17], the strain rate vector is normal to the yield surface. This concept has been further discussed in [6] where, for materials with initial work hardening and yield surfaces which are not coincident with limit surfaces, it is shown that limit state strain-rates are normal to the limit surface. Since it is materials of this nature that are considered here, the flow law for a filamentary composite can be written at a smooth point on the limit surface as

$$\bar{\varepsilon}_{ij} = \lambda \frac{\partial L^c}{\partial \bar{\sigma}_{ij}} \tag{11}$$

where $\bar{\varepsilon}_{ij}$ are the average composite limit strain rates defined so that the product $\bar{\sigma}_{ij}\bar{\varepsilon}_{ij}$ equals the rate of work in a unit volume element, L^c is the composite limit surface and λ is a positive constant of proportionality. For singular points such as corners or vertices, the strain rate vector will be a linear combination of all forms (11) which intersect at that point [19]. Geometrically, this is equivalent to requiring the strain rate vector to be within the fan or cone normals [17, 18].

Validity and limitations

It is worthwhile noting that the composite limit surface, equation (10), has been derived for arbitrary planar loading without specifying the exact limit properties of either matrix or filaments and is therefore valid for all materials exhibiting acceptable limit behavior. Anisotropic matrix behavior with unequal properties in tension and compression, etc. are all allowed. Infinite strength elastic or inextensible filaments can also be treated by letting filament limit force in tension and compression approach infinity.

The limitations on equation (10) are those outlined as assumptions, i.e. filament volume fraction and cross sectional dimensions are vanishingly small, while filament uniaxial tensile strengths are extremely large compared to matrix strength. It is noted that equation (10) can be considered as the limiting case of a volume weighted strength average as $v^m \to 1$, $v^f \to 0$, $\sigma^0 \to \infty$ and $\sigma^0 A \to f^0$ (finite) with both phases at their maximum stresses. This is similar to uniaxial tensile strength predictions by Kelly and Tyson reported in [14] and elsewhere, of unidirectional composites loaded in the fiber direction which is a true volume weighted stress average. The theory of Kelly and Tyson is applicable to tensile strength of brittle as well as ductile and short as well as long fibers. For highly ductile filaments, it coincides with that of equations (10) for uniaxial tension and $v^m \cong 1$. A volume fraction

weighted average tensile strength of unidirectional composites has been verified experimentally for both ductile and brittle fibers [1, 2, 14, for example] over a wide range of volume fractions. Conversely, for small volume fractions of fibers, it is also known that plastic tensile limit strength transverse to the filaments is that of the matrix alone. The true limit condition for v^f finite but not large should exhibit both the volume fraction weighted strength in tension along the filaments and the matrix-dominated transverse tensile strength. Equation (10) has these characteristics as shown in the next section, and is expected to give a reasonable prediction for small to moderate filament volume fractions.

The present analysis is also valid only for plastic (or infinitely strong elastic) filaments and neglects the important failure mechanisms of filament or bond rupture and interface separation. As discussed in a later section, however, the strengths predicted by equation (10) should be an upper bound to actual composite strength when filament fracture and interface separation occur.

Example–uniform filament orientation

To illustrate the procedure for computing limit surfaces from equation (10), Tresca and von Mises matrix materials reinforced with isotropic filamentary mats will be considered. The filamentary reinforcing mat is assumed to contain very many identical filaments with cross sectional area A and limit stress σ^0 in tension and compression. They are uniformly distributed angularly, such that the number of filaments/unit length between $\theta - d\theta/2$ and $\theta + d\theta/2$ is equal to $v\,d\theta$, where v is a constant. The volume fractions of fibers and matrix are, respectively,

$$v^f = \pi v A \ll 1, \qquad v^m \cong 1. \tag{12a,b}$$

The "filament alone" limit surface for this isotropic filamentary mat has been computed in [3] and is given by

$$\left[\frac{N_{11}^{Lf} - N_{22}^{Lf}}{2vf^0}\right]^2 + \left[\frac{N_{12}^{Lf}}{vf^0}\right]^2 = \cos^2\left[\frac{N_{11}^{Lf} + N_{22}^{Lf}}{2vf^0}\right]. \tag{13}$$

This surface is shown reduced by $1/t$ in Fig. 3(a), where the limit membrane forces in equal biaxial tension are $N_{11}^{Lf} = N_{22}^{Lf} = \pi v f^0$. Also shown are the Tresca [Fig. 3(b)] and von Mises [Fig. 3(c)] conditions for plane stress agreeing in uniaxial tension σ^T. Both matrix and "filament alone" limit surfaces are therefore in the form required by equation (10) for addition by normals.

To get the composite limit surfaces, choose first a strain rate vector ① (Fig. 3) with $\dot{\bar{\varepsilon}}_{11} = \dot{\bar{\varepsilon}}_{22} > 0$. By normality, this places the stress at point $\mathbf{a}^f$ of the "filament alone" and points $\mathbf{a}$ of the matrix limit surfaces which correspond to equal biaxial tension. The resulting addition of stresses is shown as points A on the Tresca [Fig. 3(d)] and the von Mises [Fig. 3(e)] matrix composite limit surfaces, also corresponding to equal biaxial tension. Next, let the strain rate vector ② be $\dot{\bar{\varepsilon}}_{11} = 0$, $\dot{\bar{\varepsilon}}_{22} > 0$. Again, the corresponding stress point on the "filament alone" surface is $\mathbf{a}^f$, but can now be anywhere on line $\mathbf{a}^t\mathbf{b}^t$ of the Tresca surface and only at point $\mathbf{b}^m$ of the Mises surface. Adding all possible stresses along $\mathbf{a}^t\mathbf{b}^t$ to stresses at $\mathbf{a}^f$ gives line $\mathbf{A}^T\mathbf{B}^T$ on the Tresca composite surface. Point $\mathbf{b}^m$ on the Mises matrix surface added to $\mathbf{a}^f$ yields point $\mathbf{B}^M$ on the Mises composite surface. Remaining points on the composite limit surfaces are found in similar fashion. It is helpful in this particular case to recognize that all cross sections of the "filament alone" and

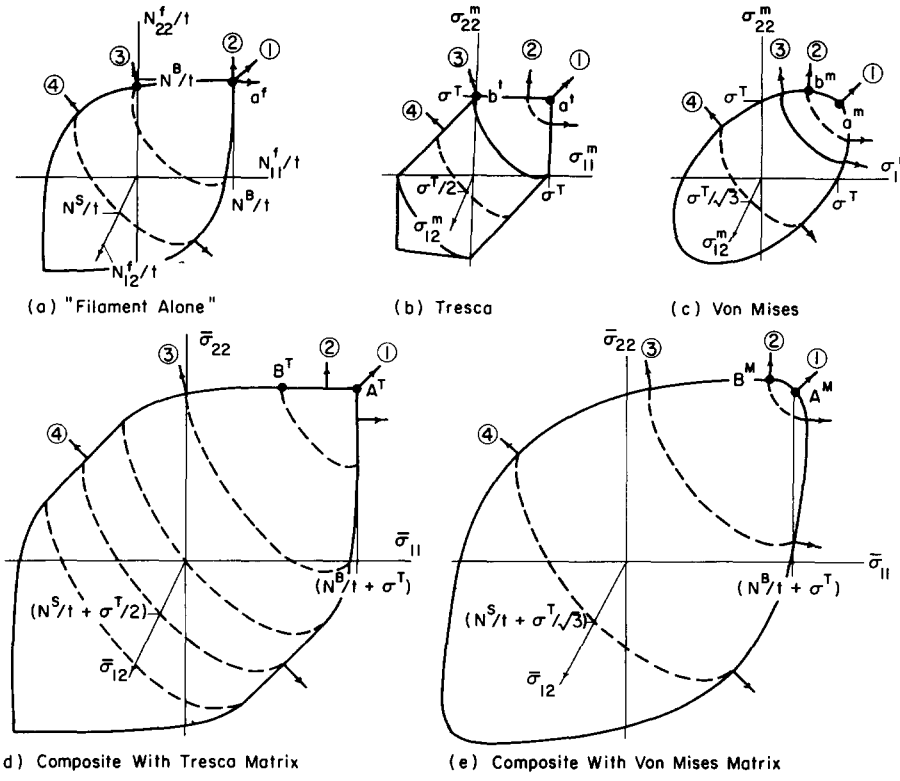

FIG. 3. Constituent limit surfaces and construction of composite limit surface for Tresca and von Mises materials reinforced with isotropic fibrous mat.

matrix surfaces perpendicular to the line $N_{11} = N_{22}$ or $\sigma_{11} = \sigma_{22}$ are concentric ellipses with ratio of major to minor axes of $\sqrt{2}$. Resulting normals to the surfaces are therefore equal at radial points on two of these ellipses having coincident normals in the 11, 22 plane as shown in Fig. 3.

Inextensible/infinite strength filaments

In the limit or collapse sense, inextensible filament reinforcement considered by Prager [10] and Helfinstine and Lance [11] is equivalent to infinite strength elastic–plastic filaments. In the former case, filaments are assumed not to extend, requiring composite extensional strains in filament directions to be zero and filament strength is assumed high enough to prevent flow or fracture of filaments.

From [3], the limit conditions for 3 or more filament families with finite limit forces are always intersecting bounded planes, giving a "filament alone" limit surface composed of $n!/(n-2)!$ flat faces. In the case of one and two family reinforcement, the surfaces are a straight line segment and a single bounded plane, respectively (Fig. 4). Matrix materials with closed, finite, plane stress limit surfaces such as those of Tresca and von Mises [Figs. 3(a), (b)], when added to any finite-sized "filament alone" surface by matching normals, will produce a composite material limit surface which is also closed and of finite size in all dimensions. It is therefore possible to have in general a normal vector to the composite

limit surface in any direction and, by normality of the strain rate vector to the limit surface, all limit state flows of finite limit force filament composites are allowed.

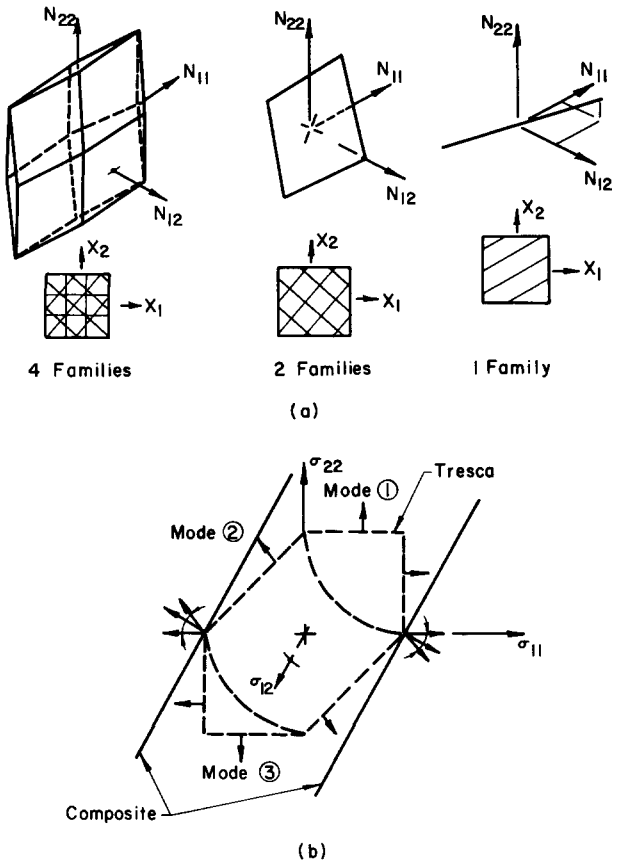

FIG. 4. (a) Typical "filament alone" limit conditions. (b) Tresca material limit condition showing deformation modes compatible with two-family infinite strength/inextensible reinforcement and resulting composite limit surface.

Consider, now, filaments of infinite limit forces in tension and compression. For three or more filament families, the "filament alone" limit surface will always enclose a three-dimensional volume of infinite extent, and will give a composite limit surface of infinite size. Limit state flow for such composites cannot occur unless composite stresses are infinite. One- and two-family infinite strength filaments, however, have surfaces with two and one, respectively, dimensions of zero size. Composite limit surfaces will therefore be an infinite-length cylinder for one family reinforcement, and two parallel infinite planes for two family reinforcement (Fig. 4). Limit state flow in these cases is restricted to those strain rate vectors which are normal to the cylinder (one family) or planes (two families). These restrictions correspond exactly to conditions imposed by inextensible fibers [10, 11], and yield specific results consistent with the general theory of Mulhern *et al.* [9 and others].

It should be mentioned that in the case of two filament family reinforcement, it is always possible to have some non-zero limit deformation at a composite stress state which

is finite as long as the matrix limit surface is finite. This conclusion is contrary to a finding by Helfinstine and Lance [11] that a two-family reinforced Tresca matrix is rigid and has infinite strengths for all possible loads. Helfinstine and Lance [11] considered the restrictions imposed by one and two families of rigid filaments and arrived at possible deformation patterns for the filamentary array alone. Upon comparing the allowable filamentary array deformations with what they termed "modes 1, 2 and 3" deformations of a Tresca material [Fig. 4(b)], they concluded that for two family reinforcement the array deformations coincided with neither of mode 1, 2 or 3 patterns. However, at the intersections of modes 1 and 2, and modes 2 and 3, a linear combination of the two deformations is allowable as shown by Koiter [19]. It is this combination of modes 1 and 2 or 2 and 3 which coincides with allowable deformations for the two family filamentary array. The combinations of modes were not included in their presentation for either one or two families of filaments, and hence their conclusions for both types of reinforcement are for the most part incorrect. It is noted, however, that since the technique used in Helfinstine and Lance was one of deformation analysis, their results are rigorous upper bounds to the exact limit surfaces.

ONE- AND TWO-FAMILY FILAMENT REINFORCEMENT

Unidirectional reinforcement

The complete limit surface for a single family of filaments with filament cross sectional area A and tensile and compressive limit stresses σ^0 and $\phi_c\sigma^0$, respectively, will now be derived. From McLaughlin and Batterman [3], the "filament alone" limit surface for a

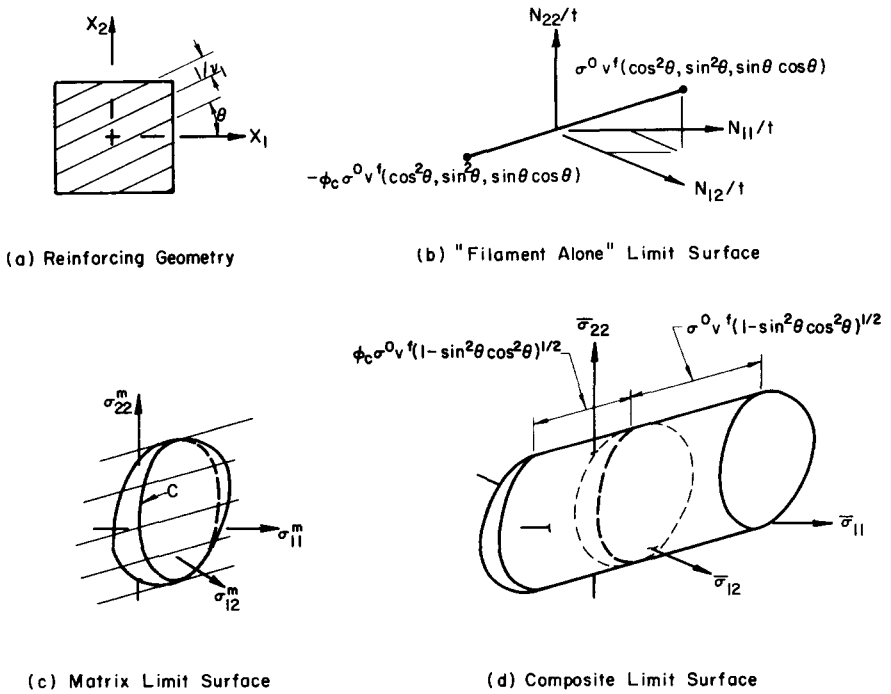

FIG. 5. Construction of composite limit surface for one family of filament reinforcement.

single family of v_1 filaments per unit length oriented at angle θ to the x_1 axis [Fig. 5(a)] is

$$\frac{N_{11}^{Lf}}{t} = \frac{fv_1}{t}\cos^2\theta$$

$$\frac{N_{22}^{Lf}}{t} = \frac{fv_1}{t}\sin^2\theta \qquad -\phi_c\sigma^0 \le \sigma^f \le \sigma^0 \tag{14}$$

$$\frac{N_{12}^{Lf}}{t} = \frac{fv_1}{t}\sin\theta\cos\theta$$

where f is the fiber force equal to $\sigma^f A$, and represents a straight line segment in stress space [Fig. 5(b)]. The matrix limit surface is arbitrary but assumed known and given by equation (3). This surface is shown schematically in Fig. 5(c).

The composite limit surface, equation (10) becomes, with (3), (14) and (1),

$$\bar{\sigma}_{11} = \overset{*}{\sigma}{}_{11}^{Lm} + \overset{*}{\sigma}{}^f v^f \cos^2\theta$$

$$\bar{\sigma}_{22} = \overset{*}{\sigma}{}_{22}^{Lm} + \overset{*}{\sigma}{}^f v^f \sin^2\theta \tag{15}$$

$$\bar{\sigma}_{12} = \overset{*}{\sigma}{}_{12}^{Lm} + \overset{*}{\sigma}{}^f v^f \sin\theta\cos\theta$$

where the star denotes stresses at points with equal normals to the respective surfaces. Graphically, this is equivalent to splitting the matrix surface in two along the curve c [Fig. 5(c)] which is the locus of all tangents to the matrix surface parallel to the "filament alone" limit line (14). The two sections are then moved in parallel to (14) by distances $v^f\sigma^0(1-\sin^2\theta\cos^2\theta)^{1/2}$ for the "front" section and $\phi_c v^f\sigma^0(1-\sin^2\theta\cos^2\theta)^{1/2}$ for the "rear" section as shown in Fig. 5(d). The resulting surface is a cylinder with generator c having an axis parallel to the "filament alone" limit line and capped by the two matrix limit surface sections. For inextensible/infinite strength filaments, the cylinder would be infinitely long in the positive and negative axial directions.

The composite limit condition can also be determined analytically. As long as filament limit stress lies in the range

$$-\phi_c\sigma^0 < \overset{*}{\sigma}{}^f < \sigma^0 \tag{16a}$$

the strain rate in both filaments and matrix must be equal and cannot have a normal component parallel to the "filament alone" limit line resulting in

$$\frac{\partial L^m}{\partial\sigma_{11}}\cos^2\theta + \frac{\partial L^m}{\partial\sigma_{22}}\sin^2 b + \frac{\partial L^m}{\partial\sigma_{12}}\sin\theta\cos\theta = 0 \tag{16b}$$

where L^m is the matrix limit surface in terms of matrix limit stress σ_{ij}^{Lm}. By use of equation (15), however, L^m and its derivatives may be put in terms of σ^f, which must obey (16a), and the desired composite limit stresses $\bar{\sigma}_{ij}$. The cylindrical portion of the composite limit condition in $\bar{\sigma}_{ij}$ space is therefore given in parametric form by the matrix limit surface (3) and the normality condition (16b) with $\overset{*}{\sigma}_{ij}$ in terms of $\bar{\sigma}_{ij}$ and $\overset{*}{\sigma}{}^f$ through (15). The filament stress $\overset{*}{\sigma}{}^f$ is restricted to be in the range (16a). It is noted that this procedure is equivalent to specifying that normal strain in the filament direction be zero for inextensible reinforcement.

For a positive normal component of strain rate in the filament direction,

$$\overset{*}{\sigma}^f = \sigma^0 \tag{17a}$$

$$\frac{\partial L^m}{\partial \sigma_{11}} \cos^2\theta + \frac{\partial L^m}{\partial \sigma_{22}} \sin^2\theta + \frac{\partial L^m}{\partial \sigma_{12}} \sin\theta\cos\theta > 0. \tag{17b}$$

The "front" end cap to the composite surface is therefore given by equation (3) with equations (15) and (17a) for all $\bar{\sigma}_{ij}$ satisfying (17b).

The "rear" end cap corresponds to a negative normal component of strain rate in the filament direction, and is given by equation (3) with equation (15) and

$$\overset{*}{\sigma}^f = -\phi_c \sigma^0 \tag{18a}$$

for all $\bar{\sigma}_{ij}$ satisfying

$$\frac{\partial L^m}{\partial \sigma_{11}} \cos^2\theta + \frac{\partial L^m}{\partial \sigma_{22}} \sin^2\theta + \frac{\partial L^m}{\partial \sigma_{12}} \sin\theta\cos\theta < 0. \tag{18b}$$

Specific composite limit conditions for matrices of von Mises and Tresca material with uniaxial tensile limit strengths σ^T are given by equations representing several intersecting surfaces as follows. The $\tilde{\sigma}_{ij}$ are non-dimensional composite stresses

$$\tilde{\sigma}_{ij} = \frac{\bar{\sigma}_{ij}}{\sigma^T} \tag{19a}$$

and η is a volume fraction–weighted ratio of matrix to filament tensile limit stresses:

$$\eta = \frac{\sigma^T}{\sigma^0 v^f}. \tag{19b}$$

von Mises matrix

$$L^c = [\tilde{\sigma}_{11}(1-\cos 2\theta) + \tilde{\sigma}_{22}(1+\cos 2\theta) - 2\tilde{\sigma}_{12}\sin 2\theta]^2 + 4[(\tilde{\sigma}_{11}-\tilde{\sigma}_{22})\sin 2\theta - 2\tilde{\sigma}_{12}\cos 2\theta]^2 - \tfrac{16}{3} = 0 \tag{20a}$$

(cylinder)

$$L^c = \tilde{\sigma}_{11}^2 + \tilde{\sigma}_{22}^2 - \tilde{\sigma}_{11}\tilde{\sigma}_{22} + 3\tilde{\sigma}_{12}^2 + \left(\frac{\Phi}{\eta}\right)^2 - 1 - \frac{\Phi}{2\eta}[\tilde{\sigma}_{11}(1+3\cos 2\theta) + \tilde{\sigma}_{22}(1-3\cos 2\theta) + 6\tilde{\sigma}_{12}\sin 2\theta] = 0 \tag{20b}$$

($\Phi = 1$ gives "front" end cap, $\Phi = -\phi_c$ gives "rear" end cap).

Tresca matrix

$$L^c = \begin{cases} [(\tilde{\sigma}_{11}-\tilde{\sigma}_{22})\sin 2\theta - 2\tilde{\sigma}_{12}\cos 2\theta]^2 - 1 = 0 & \text{(21a)} \\ [(2\tilde{\sigma}_{11} \pm 1)\sin\theta - 2\tilde{\sigma}_{12}\cos\theta]^2 + [(2\tilde{\sigma}_{22} \pm 1)\cos\theta - 2\tilde{\sigma}_{12}\sin\theta]^2 - 1 = 0 & \text{(21b)} \end{cases}$$

(cylinder)

$$L^c = \begin{cases} (\tilde{\sigma}_{11}-\tilde{\sigma}_{22})^2+4\tilde{\sigma}_{12}^2-2(\Phi/\eta)[(\tilde{\sigma}_{11}-\tilde{\sigma}_{22})+2\tilde{\sigma}_{12}\sin 2\theta] \\ \quad +(\Phi/\eta)^2-1=0 & \text{(21c)} \\ \tilde{\sigma}_{12}^2-(1\mp\tilde{\sigma}_{11})(1\mp\tilde{\sigma}_{22}) \\ \quad +(\Phi/\eta)[\mp 1+\tilde{\sigma}_{11}\sin^2\theta+\tilde{\sigma}_{22}\cos^2\theta-\tilde{\sigma}_{12}\sin 2\theta]=0. & \text{(21d)} \end{cases}$$

("Front" cap: $\Phi \pm 1$, use upper signs. "Rear" cap: $\Phi = -\phi_c$, use lower signs).

Care must be taken to choose stresses corresponding to the convex side of the double valued end cap equations, (20b) and (21c).

For inextensible/infinite strength fibers, equation (20a) is identical to the results ob-obtained by Prager [10]. As previously discussed, equations (21a)–(21d) yield significantly different results from the upper bound analysis of Helfinstine and Lance [11] due to their failure to include the plastic limit state (21b). For this same reason, the semi-empirical plastic failure theory for a one family filament reinforced material proposed by Lance and Robinson [12] is not a complete maximum shear stress (Tresca) theory and differs from equations (21).

Limit strengths for Mises and Tresca materials are shown for particular cases of simple tension, biaxial tension and tension-shear in Figs. 6 and 7. Note that composite strengths

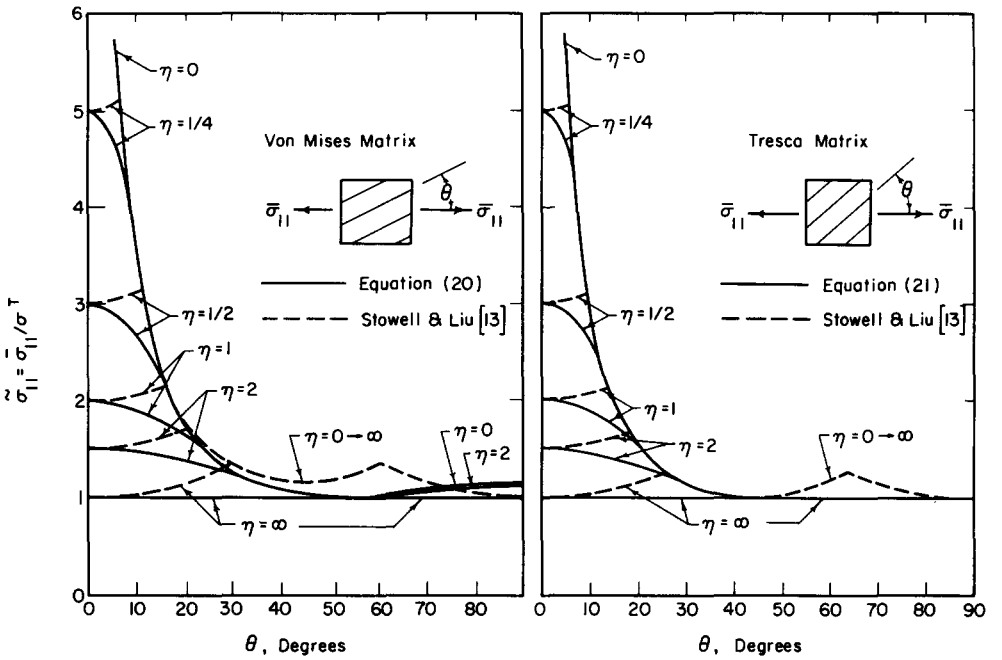

FIG. 6. Uniaxial tensile strength of Tresca and von Mises materials reinforced with one family of filaments. $\eta = \sigma^T/v^f\sigma^0$ = infinite corresponds to no reinforcement, $\eta = 0$ corresponds to infinite strength/in-extensible reinforcement.

with the Tresca matrix are always less than or equal to those with the Mises matrix. This is not surprising since the Mises limit condition circumscribes the Tresca condition for agreement in simple tension and the theorems of limit analysis [4] require limit loads from the circumscribing condition to be greater than or equal to those from the inscribing

condition. If the two limit conditions coincided in simple shear, the reverse would be true and the Tresca matrix composite would be the stronger.

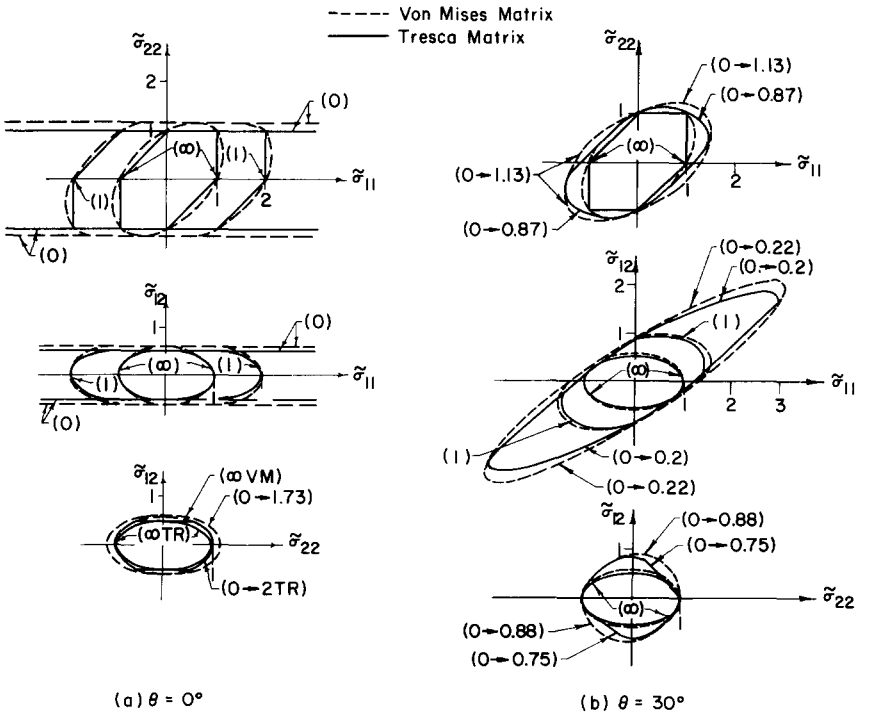

FIG. 7. Typical limit surfaces in tension-tension ($\sigma_{11}-\sigma_{22}$) and tension-shear ($\sigma_{11}-\sigma_{12}, \sigma_{22}-\sigma_{12}$) for Tresca (solid line) and von Mises (dashed line) materials reinforced with one family of filaments. Numbers in parentheses are values of $\eta = \sigma^T/v^f\sigma^0$.

The plastic strength predictions in uniaxial tension as a function of filament orientation shown in Fig. 6 for both Mises and Tresca matrices differ from the elementary prediction of Stowell and Liu [13], also shown for comparative purposes in Fig. 6. The difference is mainly for small angles of pull to the filament axis, for intermediate angles of about 10°–45° to the transverse direction, and for small amounts of reinforcement ($\eta \to \infty$). Interestingly, for no reinforcement ($\eta = \infty$), Stowell and Liu [13] would predict the matrix is stronger than itself. These differences and inconsistencies may be attributed to the non-interaction of the three failure mechanisms outlined in [13]. Most importantly, the equations of Stowell and Liu [13] may give non-conservative strength predictions for plastic materials which could result in underdesign in low factor of safety applications.

Bidirectional reinforcement

For a symmetric bidirectional array of two families of identical filaments, each with filament cross sectional area A and $v_2/2$ filaments per unit length oriented at $\pm\theta$ to the

x_1 axis [Fig. 8(a)], the "filament alone" limit surface reduces from [3], to

$$\begin{aligned} N_{11}/t &= Av_2 \cos^2\theta(\sigma_1+\sigma_2)/2 \\ N_{22}/t &= Av_2 \sin^2\theta(\sigma_1+\sigma_2)/2 \\ N_{12}/t &= Av_2 \sin\theta\cos\theta(\sigma_2-\sigma_1)/2 \\ -\phi_c\sigma^0 &\le (\sigma_1 \text{ or } \sigma_2) \le \sigma^0. \end{aligned} \tag{22}$$

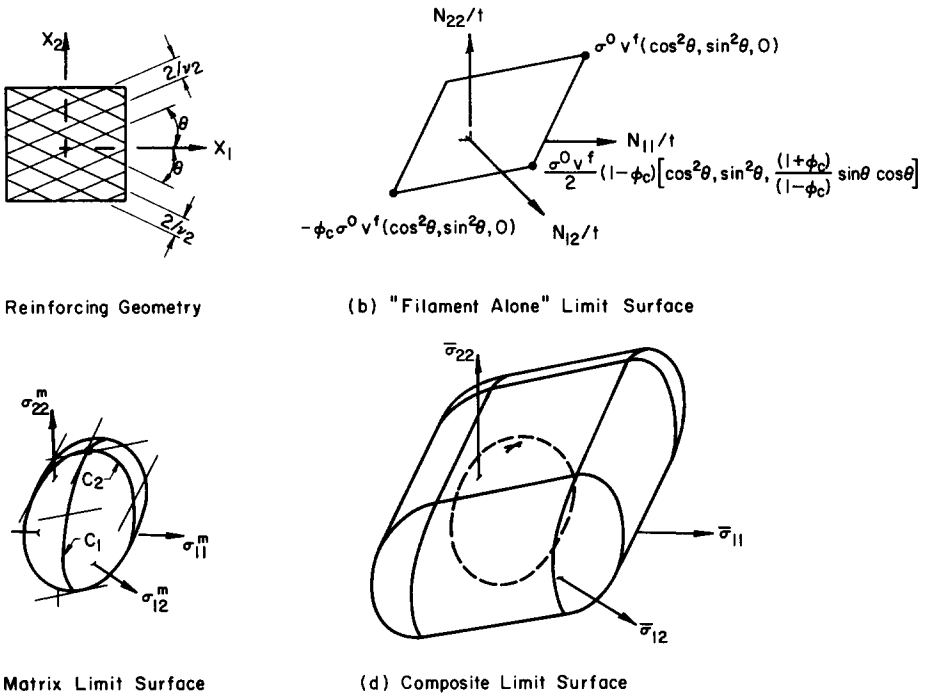

FIG. 8. Construction of composite limit surface for two families of $\pm\theta$ filament reinforcement.

Here, σ_1 and σ_2 are filament stresses at $-\theta$ and $+\theta$, respectively. For $\theta \neq 0, 90°$, equation (21) represents a single, symmetric bounded plane in stress space [Fig. 8(b)]. If $\theta = 0$ or 90°, the plane collapses to a line segment along the $x_1(0°)$ or $x_2(90°)$ axis, and results are identical to unidirectional reinforcement. Inextensible/infinite strength filaments would cause the plane or line to extend to infinity.

The procedure of adding equations (21) or Fig. 8(b) to the matrix limit surface equation (3) or Fig. 8(c) by matching normals is similar to that for unidirectional reinforcement. Here, however, the matrix limit surface must be sectioned along two curves c_1 and c_2 which are the loci of points with tangents parallel to the two directions of the lines bounding the "filament alone" plane [Fig. 8(c)]. The resulting four sections are then moved parallel to the "filament alone" lines to give the composite limit surface, Fig. 8(d). For inextensible/infinite strength filaments, the limit surface becomes two planes of infinite extent, each parallel to the lines $\bar{\sigma}_{12} = 0$ and $\bar{\sigma}_{22} = \bar{\sigma}_{11}\tan^2\theta$.

Even though the approach presented for two family reinforcement is primarily graphical for illustrative purposes, a complex analytical description of the limit criteria which closely follows that for one family reinforcement can be given. This approach, along with detailed results for bidirectional reinforcement will be given in a later paper.

Typical results for von Mises and Tresca matrix materials are shown in Figs. 9 and 10, where the non-dimensionalizations (19) have been used. Mises matrix composite results

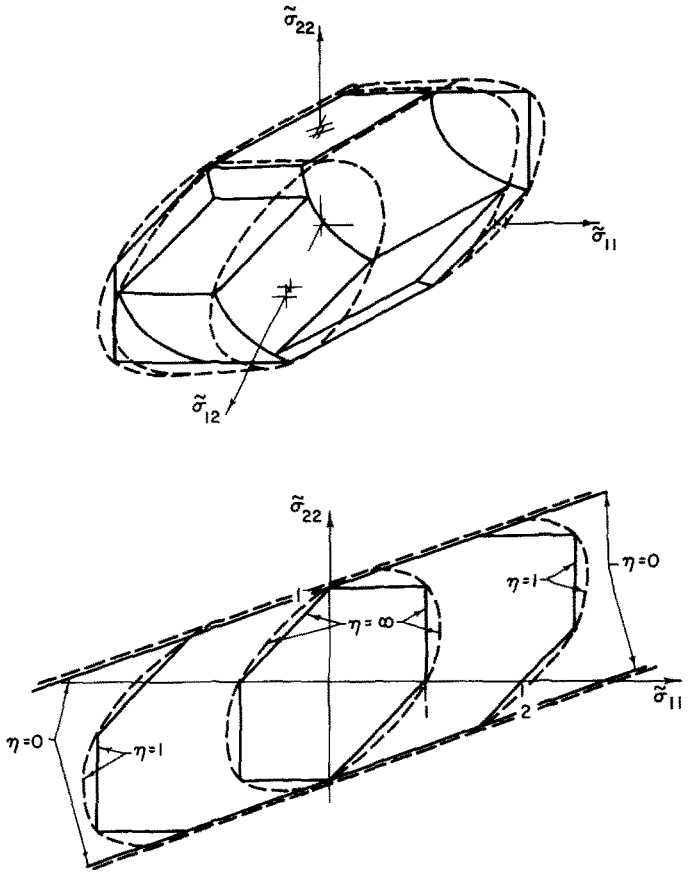

FIG. 9. Limit surfaces for Tresca (solid line) and von Mises (dashed line) materials reinforced by filaments at $\pm 30^0$ to the x_1 axis. $\eta = \sigma^T/v^f\sigma^0$.

again circumscribe Tresca matrix results for equal strengths of matrix in simple tension. Note that the three dimensional Tresca yield surface is highly complex, but simplifies greatly in biaxial tension. Comparison with the Mises matrix limit surface suggests that for general plane stress problems where errors of the order of 15 per cent or less can be tolerated, Mises matrix conditions may yield simpler solutions. For biaxial or simple tension, no clear cut advantage seems to exist other than the linearity of the Tresca criterion.

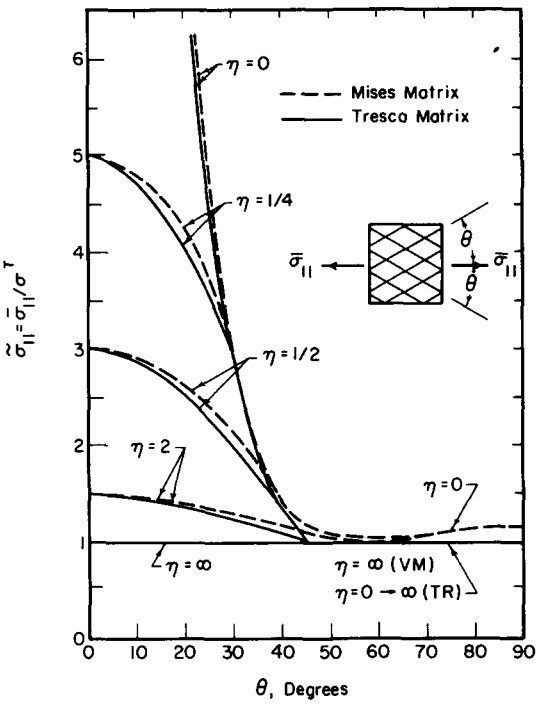

FIG. 10. Uniaxial tensile strength of Tresca and von Mises materials reinforced with two families of $\pm\theta$ filament reinforcement. $\eta = \sigma^T/v^f\sigma^0$.

Comparison with experimental results

Experiments on plastic composites involving more than one component of applied stress are unknown to the author. A study, however, was carried out by Jackson and Cratchley [20] on the tensile strength of unidirectionally and bidirectionally reinforced metals. Tests on 35 per cent stainless steel wire reinforced aluminum foil as a function of filament angle θ to direction of pull were reported for $\theta = 0$–$90°$ and are replotted on Fig. 11. The arrows imply that the data points should be moved in the direction shown for reasons of fiber reorientation and specimen damage during testing. Since neither strengths nor complete identification of the metals used were given, the composite strength of $\theta = 90°$ of about 14,000 psi was taken as σ^T, and the maximum composite strength of 120,000 psi was taken as $\sigma^T + \sigma^0 v^f$. This gave a calculated value of about 330,000 psi for σ^0 and $\eta \cong 1/8$. The agreement with the theoretical $\eta = 1/8$ curves, also plotted on Fig. 11 is good, considering experimental difficulties, for both Tresca and Mises matrices.

FAILURE BY FILAMENT, MATRIX OR BOND FRACTURE

An important aspect of this analysis has been that filaments and matrix are plastic and are allowed to reach their limit loads without fracture. Common composite failures, however, may be due in large part to filament or matrix fracture, bond failure or interface separation. While the present analysis cannot predict these rather complex phenomena, the relationship between fracture loads and loads predicted by the limit analysis will be discussed.

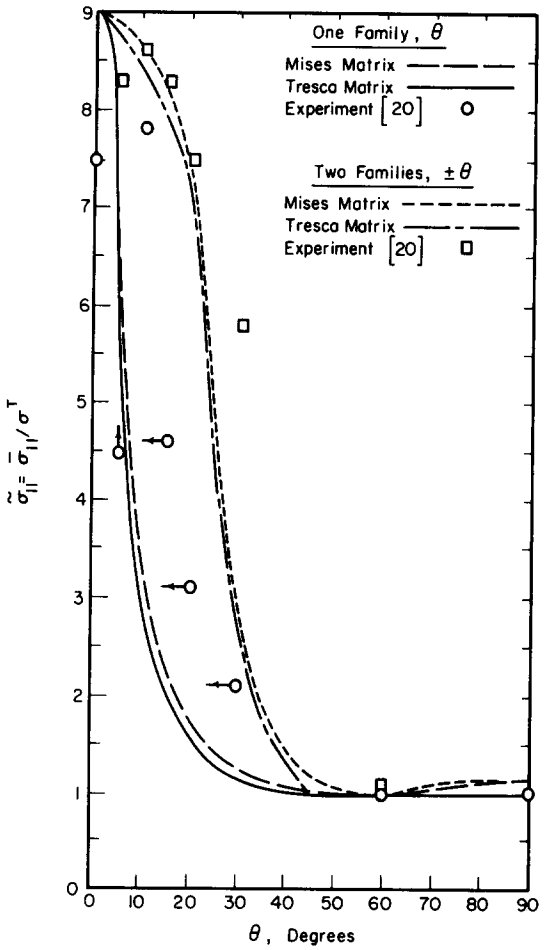

FIG. 11. Comparison of analytical results with tensile strength of steel wire reinforced aluminum from Jackson and Cratchley [20].

The description of "filament alone" limit conditions presented in [3] shows that at the limiting state, filaments are either at their limit forces in tension or compression or at a lesser force which allows deformation to occur in a representative structural element with no increase in load. It is impossible to increase the applied load in a representative structural element beyond the limit state for given ratios of applied membrane stresses by a redistribution of filament forces. Fracture of filaments at or before their limit load can therefore only serve to decrease the maximum load carrying capacity of the RSE.

In the present analysis, both filaments and matrix are at their limit stresses everywhere throughout the composite RSE when the maximum (limit) load on the composite is reached. Filament or matrix fracture or phase bond failure under filament or matrix stresses which are at or below the respective limit state therefore requires composite stresses to be at or below the composite limit state. Composite limit strengths presented herein should therefore be an upper bound to failure strengths of composites where fracture of filaments, matrix, bonds and/or interface separation can occur.

The upper bound to composite strength computed by this method should be closest to actual behavior for materials of high ductility and bond strengths. It is emphasized, however, that fibers need not exhibit any ductility for this upper bound concept to hold. An upper bound to true failure criteria for composites with fibers of carbon, glass or boron in epoxy or metal matrices can therefore be computed by setting the filament limit stress σ^0 equal to the filament fracture stress. Since fibers of this ilk are usually much stiffer than the matrix, filament fracture should occur under certain loading conditions, such as simple tension in the filament direction, well before maximum matrix stresses are reached. True failure loads for these cases are therefore expected to be significantly lower than loads predicted from the limit analysis.

CONCLUSIONS

A method for computing plane stress limit behavior of plastic filament reinforced materials is presented herein. Both limit conditions or maximum plastic strength and flow laws are discussed for arbitrary material limit behavior and filament orientation. While the equations are analytically valid for small volume fractions of high strength filaments in a much weaker matrix, such experimental evidence as exists appears to corroborate the theory, at least approximately, for moderate filament volume fractions. The analysis gives results which are consistent with established analytical results of other researchers for their specific material behavior and reinforcing filament geometry. Although mechanisms of fiber fracture, matrix fracture, bond failure and interface separation are not predicted, the limit conditions should be upper bounds to the strength of composites which fail by those means.

The present analysis is not valid for high volume fractions of filaments, nor for matrix strengths which approach those of the filaments. Work is currently underway to evaluate the effects of these conditions.

Acknowledgements—This work has been supported under National Science Foundation Grant NSF-GK-5582 to the University of Illinois, for which the author is grateful. The author also wishes to thank Mr. Saurindranath Majumdar for performing much of the computational work presented herein.

REFERENCES

[1] D. CRATCHLEY, Experimental aspects of fibre-reinforced metals. *Metall. Rev.* **10**, 79–144 (1965).
[2] A. KELLY and G. J. DAVIES, The principles of the fiber reinforcement of metals. *Metall. Rev.* **10**, 1–77 (1965).
[3] P. V. MCLAUGHLIN, JR. and S. C. BATTERMAN, Limit behavior of fibrous materials. *Int. J. Solids Struct.* **6**, 1357–1376 (1970).
[4] D. C. DRUCKER, W. PRAGER and H. J. GREENBERG, Extended limit design theorems for continuous media. *Q. appl. Math.* **9**, 381–389 (1952).
[5] P. V. MCLAUGHLIN, JR. and S. C. BATTERMAN, On extending the range of applicability of the limit theorems. *J. appl. Mech.* **37**, 518–521 (1970).
[6] P. V. MCLAUGHLIN, JR., Properties of work-hardening materials with a limit surface. *J. appl. Mech.* to appear.
[7] Z. HASHIN, Transverse strength of fibrous composites, Evaluation of Filament Reinforced Composites for Aerospace Structural Applications, NASA CR-207 (1965).
[8] L. S. SHU and B. W. ROSEN, Strength of fiber-reinforced composites by limit analysis methods. *J. Composite Mater.* **1**, 366–381 (1967).
[9] J. F. MULHERN, T. G. ROGERS and A. J. M. SPENCER, A continuum theory of a plastic–elastic fibre-reinforced material. *Int. J. Engng Sci.* **7**, 129–152 (1969).
[10] W. PRAGER, Plastic failure of fiber-reinforced materials. *J. appl. Mech.* **36**, 542–544 (1969).

[11] J. D. HELFINSTINE and R. H. LANCE, Yielding of a Fiber Reinforced Tresca Material, Presented at ASCE-EMD Specialty Conference, Mechanics Research in Civil Engineering, University of Illinois at Urbana-Champaign (1971).
[12] R. H. LANCE and D. W. ROBINSON, A maximum shear stress theory of plastic failure of fiber-reinforced materials. *J. Mech. Phys. Solids* **19**, 49–60 (1971).
[13] E. Z. STOWELL and T. S. LIU, On the mechanical behavior of fibre-reinforced crystalline materials. *J. Mech. Phys. Solids* **9**, 242–260 (1961).
[14] A. KELLY and W. R. TYSON, Tensile properties of fibre-reinforced metals: copper tungsten and copper/molybdenum. *J. Mech. Phys. Solids* **13**, 329–350 (1965).
[15] V. D. AZZI and S. W. TSAI, Anisotropic strength of composites. *Exp. Mech.* **5**, 283–288 (1965).
[16] C. C. CHAMIS, Failure Criteria for Filamentary Composites, *Composite Materials: Testing and Design*, pp. 336–351. A.S.T.M. (1969).
[17] D. C. DRUCKER, A More Fundamental Approach to Plastic Stress-Strain Relations, *Proceedings of the First National Congress of Applied Mechanics*, pp. 487–491, American Society of Mechanical Engineers, New York, (1951); D. C. DRUCKER, On the postulate of stability of material in the mechanics of continua. *J. Méc.* **3**, 235–249 (1964); D. C. DRUCKER, Plasticity, *Structural Mechanics*, pp. 407–455. Pergamon Press (1960).
[18] R. HILL, The essential structure of constitutive laws for metal composites and polycrystals. *J. Mech. Phys. Solids* **15**, 79–95 (1967).
[19] W. T. KOITER, Stress–strain relations, uniqueness and variational theorems for elastic–plastic materials with a singular yield surface. *Q. appl. Math.* **11**, 350–354 (1953).
[20] P. W. JACKSON and D. CRATCHLEY, The effect of fibre orientation on the tensile strength of fibre-reinforced metals. *J. Mech. Phys. Solids* **14**, 49–64 (1966).

(*Received* 7 *October* 1971)

Абстракт—Используя предельный анализ для произвольно плоских решеток из тонких, сильных волокон, находящихся в матрице более слабых материалов, определяются предельные условия плоских напряжений или зоны максимального пластического сопротивления. Предполагается что как волокна так и матрица пластические, с допускаемым предельным поведением, но относительные предельные условия произвольны. Граничный случай обьемного разрыва, со средным взвешенным, для составной фазы граничных напряжений, предсказанное для пластического сложного сопротивления. Оно должно быть, также, верхним пределом по сравнению со сопротивлением составных материалов с хрупкими волокнами, или где излом может появиться другим способом. Даются специфические результаты для усиления в одном направлении или в двух. Они соглашаются с зкспериментом.